MÖSSBAUER STUDY OF SMALL-PARTICLE MAGHEMITE

P.M.A. de BAKKER [1], E. De GRAVE [1,*], R.E. VANDENBERGHE [1] and L.H. BOWEN [2]

[1] *Laboratory of Magnetism, Gent State University, Proeftuinstraat 86, B-9000 Gent, Belgium*
[2] *Department of Chemistry, North Carolina State University, Box 8204, Raleigh, NC 27695, U.S.A.*

Two small-particle maghemite (γ-Fe_2O_3) samples have been investigated with the Mössbauer effect. From the results of the model-independent hyperfine-field distribution fits some characteristic temperature-dependent parameters have been obtained. The spectra at the lowest temperatures could be fitted with two strongly overlapping hyperfine-field distributions with different isomer shifts. Spectra in applied magnetic fields ranging from 40 to 60 kOe, and at 4.2 K showed non vanishing $\Delta m_I = 0$ absorption lines. The hyperfine-field distribution and canting-angle distribution method for fitting these spectra did not yield reasonable results. Therefore, a bi-dimensional hyperfine-field-canting-angle distribution has been applied, and was found to reproduce the experimental line shapes with remarkable adequacy. The resulting distribution profiles revealed a linear correlation between H_{hf} and the angle between the magnetic moments and the external field.

It is well known that lepidocrocite (γ-FeOOH) upon heating in air, first decomposes into maghemite (γ-Fe_2O_3) which at higher temperatures transforms into hematite (α-Fe_2O_3). TGA and DSC measurements of the two single-phase, but poorly crystalline γ-FeOOH samples (labeled L121 and L147, with the digits referring to the specific surface area in m^2/g as obtained by BET measurements), yielded similar curves. The loss of weight, starting at about 200 °C, marks the endothermic γ-FeOOH to γ-Fe_2O_3 transition. The γ-Fe_2O_3 to α-Fe_2O_3 exothermic transition temperature is approximately 430 °C.

The obtained decomposition products were characterized with transmission electron microscopy (TEM), X-ray diffraction (XRD) and Mössbauer spectroscopy (MS). The TEM photographs of the γ-Fe_2O_3 samples revealed large conglomerates of very small needle-like shaped crystallites. This clustering is due to the magnetic coupling of the ferrimagnetic particles [1]. XRD measurements of the two selected maghemite samples (labeled L121-303 and L147-311, with the last digits referring to the annealing temperature in air of the parent lepidocrocite for one hour) showed very broad diffraction peaks, indicating a low degree of crystallinity. The values for the mean crystallite diameter (MCD) along certain crystallographic directions, as estimated from the full width at half maximum

* Senior Research Associate at the National Fund for Scientific Research, Belgium.

Table 1
Average hyperfine field $\overline{H}_{hf}$, field of maximum probability H_{hf}^{m}, quadrupole shift 2ϵ and isomer shift δ (relative to metallic iron) of the hyperfine field distributions fitted to the spectra at 80 K and RT of the maghemite samples. For comparison, literature data for single phase, well crystalline maghemite are given as well (single sextet fit).

Sample	80 K				RT			
	$\overline{H}_{hf}$ (kOe)	H_{hf}^{m} (kOe)	2ϵ (mm/s)	$\delta^{(Fe)}$ (mm/s)	$\overline{H}_{hf}$ (kOe)	H_{hf}^{m} (kOe)	2ϵ (mm/s)	$\delta^{(Fe)}$ (mm/s)
γ-Fe_2O_3	517		$\cong 0.00$	0.40	500		$\cong 0.00$	0.32
L121-303	479	498	0.01	0.44	274	368	−0.00	0.30
L147-311	465	489	−0.01	0.44	226	318	0.01	0.36

(FWHM) of the corresponding diffraction lines using the Scherrer formula, are generally smaller than 10 nm.

The temperature-dependent Mössbauer spectra of both maghemite samples consist of a broad sextet distribution and a superimposed central doublet distribution for $T \geqslant 160$ K for sample L121-303 and for $T \geqslant 130$ K for sample L147-311. The central doublet component is due to the fraction of γ-Fe_2O_3 particles which are superparamagnetic at the considered temperature. The spectra have been described by a model-independent magnetic hyperfine-field distribution (MHFD) based on the method of Wivel and Mørup [12] and, when necessary, an additional quadrupole splitting distribution (QSD). The hyperfine parameters at RT and 80 K for the sextet components of the investigated maghemites are listed in table 1 and literature data for acicular maghemite particles [2] have been included as well. The relative contribution of the QSD to the total spectrum gradually increases with increasing temperature from 3% at 160 K to 35% at 400 K for sample L121-303, and from 10% at 130 K to 95% at 400 K for sample L147-311. These data, however, are not very accurate due to the strong overlap with low-field magnetic components. From extrapolation of the linear part of the curve representing the relative doublet area as a function of the measuring temperature to 0%, the blocking temperature T_B for the present maghemite samples is estimated to be 160 K for L121-303 and 130 K for L147-311, which is in good agreement with the results obtained by Picone et al. [3] and by Coey and Khalafalla [5] for maghemites with average particle size of respectively 7.5 and 6.5 nm.

From the low-temperature Mössbauer spectra the broad hyperfine-field distribution reflects a wide range in particle size with a very low average volume. For such an ultrasmall-particle system, intra-particle collective magnetic excitations [5] and inter-particle magnetic interactions [6] reduce the H_{hf} of an individual particle by an amount depending on its volume to fields anywhere between zero and the maximum value that can be expected at that temperature. At low temperatures, the peak depths of the outer absorption lines are clearly asymmet-

Table 2
Numerical deconvolution of the two strongly overlapping hyperfine field distributions of maghemite at different temperatures. The absorption areas have been fixed to a 3:2:1 ratio.

Sample	T (K)	$\overline{H}_{hf}$ (kOe)	H_{hf}^{m} (kOe)	2ϵ (mm/s)	$\delta^{(Fe)}$ (mm/s)	Area (%)
L147-311	5	481	501	−0.029	0.344	30.3
		510	514	−0.007	0.474	69.7
L121-303	12	484	502	−0.036	0.349	26.6
		515	521	−0.002	0.460	73.4
	30	486	501	−0.034	0.366	36.8
		514	518	−0.010	0.463	63.2
	55	481	502	−0.035	0.381	48.5
		511	516	0.000	0.466	51.5

ric, which is not reproduced in the calculated spectrum. This asymmetry arises from the existence of two MHFD's with unequal isomer shifts, corresponding to A- and B-site ferric ions. Indeed, maghemite is a spinel with formula $(Fe)_A(Fe_{5/3}\square_{1/3})_BO_4$, where A and B stand for tetrahedral and octahedral sites respectively, and vacancies are denoted by □. The difference in δ values is generally too small (i.e. $\delta_B - \delta_A \cong 0.1$ mm/s) to enable a numerical deconvolution of the temperature-dependent spectra into two separate, but, strongly overlapping distributions except for the spectra recorded at the lowest temperatures (4.2 K up to 55 K) as indicated in table 2.

In order to obtain a better resolution of the two sublattice spectra, we recorded spectra of L147-311 and L121-303 at 4.2 K and 10 K respectively, in an external magnetic field H_{ext} of different strength, applied parallel with the γ-ray direction. If the magnetic structure is collinear, the $\Delta m_I = 0$ absorption lines are expected to be absent. This is, however, not the case, as can be seen in fig. 1. These non-vanishing lines can be explained by assuming non-collinearity of the spins: the angle θ between the intrinsic hyperfine-field H_{hf} and H_{ext} is different from 0 (A-sites) or 180 (B-sites) degrees. Possible explanations for the non-vanishing intensities are: spin canting in the surface layers ("pinning") [7] or incomplete alignment of the particles' magnetization vector due to strong anisotropy effects (uniaxial shape anisotropy) or to interactions of the particles' magnetic moment with the average magnetization of surrounding particles [8]. The effective hyperfine-field ($\boldsymbol{H}_{eff} = \boldsymbol{H}_{ext} + \boldsymbol{H}_{hf}$) distribution or canting-angle distribution method for fitting this latter spectrum did not yield a reasonable goodness-of-fit. Therefore we tried another approach for the analysis of the external-field spectra: a simultaneous distribution in the angle θ and the hyperfine-field H_{hf}. The bi-dimensional distribution approach, based on matrix inversion [9], gives rise to remarkably good fitting results (see fig. 1). The results for the different fitting methods are given in table 3 indicating that (a) the isomer shift $\delta^{(Fe)}$ and the quadrupole shift 2ϵ do not depend on the fitting model, whereas (b) the relative

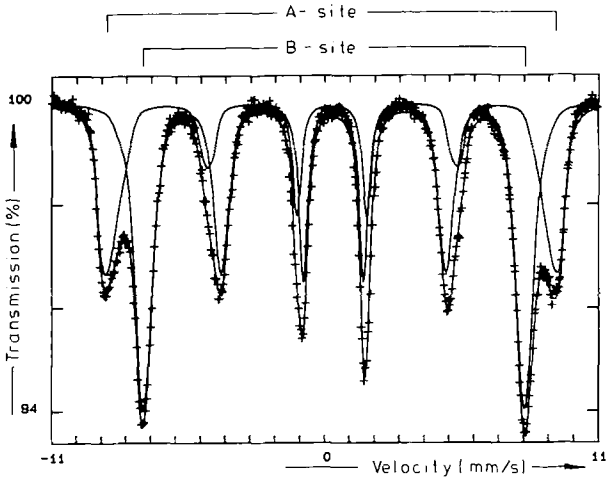

Fig. 1. Maghemite (sample L121-303) at 10 K in an external field of 60 kOe fitted with a bi-dimensional H_{hf}-θ distribution for A and B sites.

absorption areas of A- and B-sites do. As there is no superstructure present at the B-sublattice [10], the calculated relative areas of A and B sublattices are given by: $S_A = 37.5\%$ and $S_B = 62.5\%$. The experimental values S_A and S_B obtained by the double-distribution method, are closest to the theoretical values. The results obtained for the maghemite sample L147-311 are similar to those for sample L121-303 except for the $H_{ext} = 40$ kOe spectrum where the relative areas of A-

Table 3
Results of the different distribution fits for the two maghemite samples under different conditions of temperature and external field. (a) H_{eff} distribution, (b) θ distribution with fixed values for the intrinsic hyperfine fields at A and B sites ($H_{hf}^{A} = 511$ kOe, $H_{hf}^{B} = 552$ kOe) and (c) double distribution approach.

Sample	Site	T (K)	H_{ext} (kOe)	$\overline{H}$* (kOe)	H^m* (kOe)	$\bar{\theta}$ (°)	θ^m (°)	$\delta^{(Fe)}$ (mm/s)	2ϵ (mm/s)	Area (%)	χ^2
L121-303	A [a]	10	60	558	571			0.385	−0.040	32.2	4261
	B [a]			480	477			0.477	0.008	67.8	
	A [b]					–	37	0.387	−0.070	52.4	5018
	B [b]					–	138	0.476	0.018	47.6	
	A [c]			505	513	37	32	0.380	−0.062	35.9	1609
	B [c]			518	525	137	140	0.475	0.006	64.1	
L147-311	A [c]	4	40	487	464	52	54	0.370	−0.020	56.3	
	B [c]			518	526	134	143	0.442	−0.320	43.7	
	A [c]		55	498	512	45	40	0.386	−0.048	38.1	
	B [c]			518	527	133	138	0.481	0.001	61.2	

* For (a) $\overline{H}$ and H^m represent the average and maximum effective hyperfine field H_{eff}, whereas for (c), $\overline{H}$ and H^m represent the average and maximum intrinsic hyperfine field H_{hf} for A and B sites.

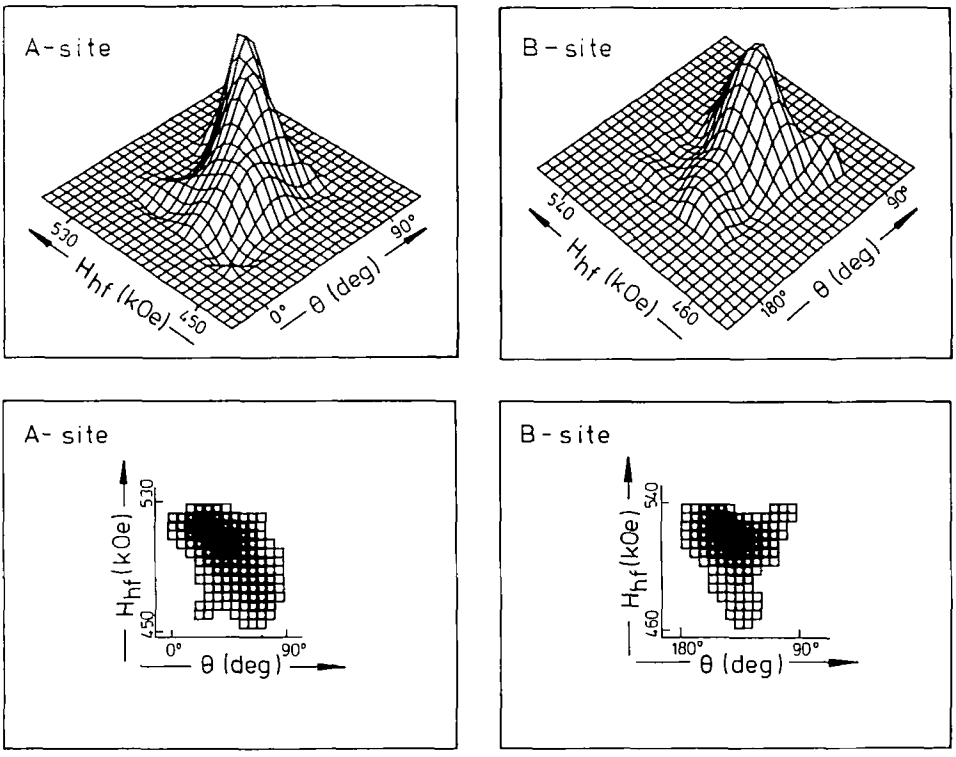

Fig. 2. Two representations for the bi-dimensional distribution profiles for A and B sites of sample L121-303, showing the possible correlation between H_{hf} and θ.

and B-sublattices deviate substantially from the ideal values. This is due to the still insufficient separation of A and B subspectra when an external field of 40 kOe is applied. The obtained bi-dimensional distribution profiles, depicted in fig. 2 for sample L121-303, show a possible correlation between H_{hf} and θ. High H_{hf} values correspond to small deviations of the complete alignment of the hyperfine field along H_{ext}. Consider for example a particle with predominant uniaxial shape anisotropy originating from microscopic effects at the Fe^{3+}-ions. There is undoubtedly a distribution in the strength of this microscopic anisotropy when going from the inner part of the particle to the surface. Furthermore, the magnetic hyperfine-field at the Fe^{3+}-ions in the particle is also distributed due to, for example, field reduction in the surface layers, which was proven to occur in the case of an uncharacterized Fe_2O_3 film at room temperature [11]. The existence of a H_{hf} distribution can also be derived from the spectra in zero applied field which indicate such distribution even at 4.2 K. When an external field H_{ext} is applied, making an angle α with the easy axis of the microscopic uniaxial anisotropy, the magnetic hyperfine-field at the Fe^{3+} ions will not align completely but make an angle θ with the γ-ray direction provided that the strength of the microscopic uniaxial anisotropy has values comparable with the strength ex-

ercised by the external field. The distribution of the magnetic hyperfine field and the uniaxial anisotropy then determines the distribution of the angle θ, giving rise to the observed correlation between H_{hf} and θ. At present, the results of this bi-dimensional approach are still in an exploratory stage and many other magnetic systems under various external conditions (external-field strength, temperature, etc...) ought to be considered to assess the validity of the fitting model.

Acknowledgments

This work was supported in part by the Fund for Joint Basic Research (Belgium) and by a NATO collaborative Research Grant 0370/86. The assistance of Prof. Dr. R. Vochten and Dr. W. Bohyn is greatly acknowledged.

References

[1] A.E. Berkowitz, W.J. Schuele and P.J. Flanders, J. Appl. Phys. 39 (1968) 1261.
[2] K. Haneda and A.H. Morrish, Phys. Lett. 64A (1977) 259.
[3] P.J. Picone, K. Haneda and A.H. Morrish, J. Phys. C: Solid State Phys. 15 (1982) 317.
[4] J.M.D. Coey and D. Khalafalla, Phys. Status Solidi (a) 11 (1972) 229.
[5] S. Mørup and H. Topsøe, Appl. Phys. 11 (1976) 63.
[6] S. Mørup, J. Magn. Magn. Mater. 37 (1983) 39.
[7] A.H. Morrish, K. Haneda and P.J. Schurer, J. Phys. Colloq. 37 (1976) C6-301.
[8] E. Tronc and D. Bonnin, J. Phys. Lett. 46 (1985) L437.
[9] P. Levitz, D. Bonnin, G. Calas and A.P. Legrand, J. Phys. E: Sci. Instrum. 13 (1980) 427.
[10] K. Haneda and A.H. Morrish, Solid State Commun. 22 (1977) 779.
[11] T. Yang, A. Krishnan, N. Benczer-Koller and G. Bayreuther, Phys. Rev. Lett. 48 (1982) 1292.
[12] C. Wivel and S. Mørup, J. Phys. E: Sci. Instrum. 14 (1981) 605.